Vol. **111** (2007) *ACTA PHYSICA POLONICA A* No. 4

Proceedings of the XII National School "Correlated Electron Systems...", Ustroń 2006

# Kondo Insulating State in $CeRhSb_{1-x}Sn_x$ as a Function of Carrier Number and Its Subsequent Metallization

A. Ślebarski[a] and J. Spałek[b]

[a]Institute of Physics, University of Silesia
Uniwersytecka 4, 40-007 Katowice, Poland
[b]Marian Smoluchowski Institute of Physics
Jagiellonian University, Reymonta 4, 30-059 Kraków, Poland

A quantum critical point represents an essential singularity in the phase diagram of the electron-correlated compounds. In the $CeRhSb_{1-x}Sn_x$ system we have observed a quantum criticality at the boundary Kondo insulator–non-Fermi liquid state. In this series of compounds, CeRhSb has a Kondo insulating ground state, whereas CeRhSn exhibits a non-Landau Fermi liquid behavior. In view of different types of behavior of CeRhSb and CeRhSn, we review the results of the solution in $CeRhSb_{1-x}Sn_x$ and discuss the effect of a quasi-continuous change of the number of conduction electrons on the gap formation in the Kondo-insulating regime, as well as on the critical behavior appearance near the quantum critical point.

PACS numbers: 71.27.+a, 72.15.Qm, 71.30.+h

## 1. Introduction

In the last four decades of research on the *strongly correlated electron systems*, the studies evolved from the dilute Kondo systems [1, 2], and fluctuating valence systems [3], heavy fermion (HF) systems [4], and HF superconductors [5] to the Kondo insulators (KI) [6] and non-Fermi liquid (NFL) systems [7]. In the last decade, the interest grew in the strongly correlated compounds, which display the *critical quantum behavior* [8]. In particular, attention focused on the Ce or U compounds which at $T = 0$ undergo a quantum phase transition as a function of tuning parameter $x$ such as concentration of defects or impurities [9–12], external pressure [13, 14], and magnetic/electric field [15].

A quantum critical point (QCP) is a singular point on the phase diagram, e.g., on the concentration ($x$)–temperature ($T$) plane at a critical concentration

$x = x_c$ and $T = 0$, where the characteristic energy scale $k_B T(x)$ of quantum excitations approaches zero (it is, e.g., a new state of matter, where the wave function becomes an entangled mixture of the ordered and disordered states, see e.g. [16]). The presence of a singular quantum critical point at absolute zero induces an unusual metallic behavior over an extended range of temperature, in which real experiments are carried out, so the question is what are the consequences of the transition at $T = 0$ for physical properties at $T > 0$. In the low-$T$ range, as the QCP is approached, the electronic specific-heat coefficient $\gamma \equiv C(T)/T$ has a singular behavior, indicating a divergence in the effective mass $m^*$ with $T \to 0$. The indefinite $C(T)/T$ value (e.g., $C/T \propto -\ln T$ or $C/T \propto T^{-n}$), and other deviations from the Landau–Fermi-liquid behavior for the magnetic susceptibility $\chi$ behavior as $T \to 0$ and the electrical resistivity $\rho$ are clearly seen (for an overview, see Refs. [7, 17]). In particular, the electrical resistivity changes as $\Delta\rho \propto T^{\varepsilon}$ with exponents $1 \leq \varepsilon < 2$ and the magnetic susceptibility varies as $T^{-n}$ or $\chi \propto -\ln T$. There exist NFL materials, for which $\rho$, $C/T$, and $\chi$ do not all conform the expected NFL behavior, i.e., logarithmic or power-law divergent behavior which extends over several decades on $T$ scale. For example, in $Y_{1-x}U_xPd_3$, the first $f$-electron system in which NFL behavior was identified [18], and in $YbRh_2Si_2$ [19], $C(T)/T$ exhibits an upward departure from $-\ln T$ dependence at lower temperatures, while $\rho(T)$ remains linear in $T$ throughout the whole range.

There is a growing number of HF materials that can be placed as those in the vicinity of a quantum critical point and can be tuned to QCP by alloying, e.g. $CeCu_{6-x}Au_x$ [10], through the direct application of pressure [13] (the case of $CeIn_3$), or via the application of the magnetic field [15], as in the case of $YbRh_2Si_2$. Most published results concerning the QCP in the Kondo-lattice systems were obtained with disordered systems, as discussed below for the series $Ce_{1-x}La_xRhSn$ of compounds [20, 21]. Very recently, we have reported novel quantum criticality at the border of *Kondo insulator–non-Fermi liquid* in the correlated-electron system $CeRhSb_{1-x}Sn_x$, detected as a function of number of valence electrons in the system [22].

The aim of this brief review is to present and discuss this new type of quantum critical behavior for $CeRhSb_{1-x}Sn_x$.

## 2. Stabilization of the collective Kondo semiconducting state by Sb doping in $CeRhSb_{1-x}Sn_x$

CeRhSn displays a NFL metallic character of the low-temperature physical properties [23], which were interpreted in terms of the Griffiths phases [24]. This model predicts a power-law behavior of $C(T)/T$ and $\chi(T)$ with the similar values of the exponents. The values of the power-law exponent 1/2 obtained from the $C(T)/T$ and $\chi(T)$ experimental data [23] are in reasonable agreement with experiment, suggesting that the NFL behavior can be described by the Griffiths model, which means that the static disorder plays an important role. In Fig. 1

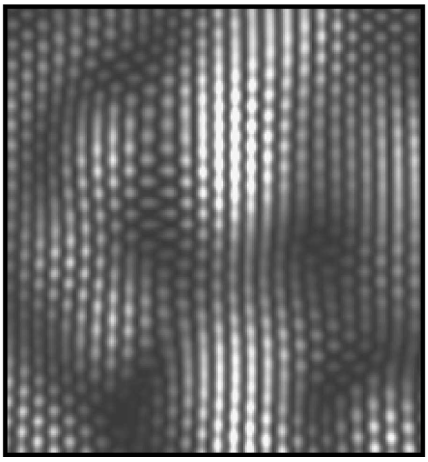

Fig. 1. STM image from a small part $\approx 20 \times 20$ nm$^2$ of surface. The image topology contains clusters, dislocations, and point defects.

we present the scanning tunneling microscopy (STM) image of the small part of CeRhSn surface with an atomic resolution (for details see Ref. [25]), which indeed shows the presence of atomic clusters and atomic defects.

In consequence, the ac susceptibility $\chi_{\rm ac}$ shows a well-defined peak at $\approx$ 10 K [26] characteristic of spin-glass formation and the power-law behavior at $T < 10$ K, which suggest that CeRhSn can be regarded as the system close to QCP. In order to characterize further the NFL behavior close to QCP, we have investigated the magnetic properties of $Ce_{1-x}La_xRhSn$ series [21]. It was found that the substitution of La for Ce suppresses the spin-glass ordering at $x_{\rm c} \approx 0.5$ (see Fig. 2).

Additionally, as shown in Fig. 2, $\Delta\chi \sim T^{-n}$ and $\Delta C/T \sim -\ln T$ (resistivity $\rho(T) \sim T$, Ref. [21]) around the critical concentration. However, the nature of the NFL behavior at both sides of the critical concentration $x_{\rm c}$ is different. Namely, for $x > x_{\rm c}$ (i.e., on the La-rich side) the magnetic properties of $Ce_{1-x}La_xRhSn$ are dominated by the existence of spin fluctuations, whereas on the Ce-rich side spin clusters can be formed and are analogous to Griffiths phases (see Fig. 3).

We now turn to the $CeRhSb_{1-x}Sn_x$ system. CeRhSb represents a rare example of cerium-containing HF Kondo insulator with a narrow energy gap [27, 28] of $\approx$ 7 K. As we have reported [22], the system $CeRhSb_{1-x}Sn_x$ with growing $x$ exhibits a quantum transition from the Kondo-insulator to the non-Fermi (non--Landau) metallic state of correlated electrons. The QPC is located at $x_{\rm c} \approx 0.12$, i.e., on the Sb-rich side. In the Sb-rich regime, we observed for the samples $x \leq 0.12$: (i) the activated behavior of the conductivity ($\rho \sim \exp(\Delta/k_{\rm B}T)$) and $\chi_{\rm ac} \to 0$ with $T \to 0$, and (ii) a novel type of scaling $\rho\chi = {\rm const}$ (see Fig. 4).

The observed scaling law $\rho \sim \chi^{-1}$ at low $T$ can be understood in an elementary manner by recalling the Drude formula $\rho = m^*/(n_{\rm c}e^2\tau)$, as well as $\chi \sim n_{\rm c}$

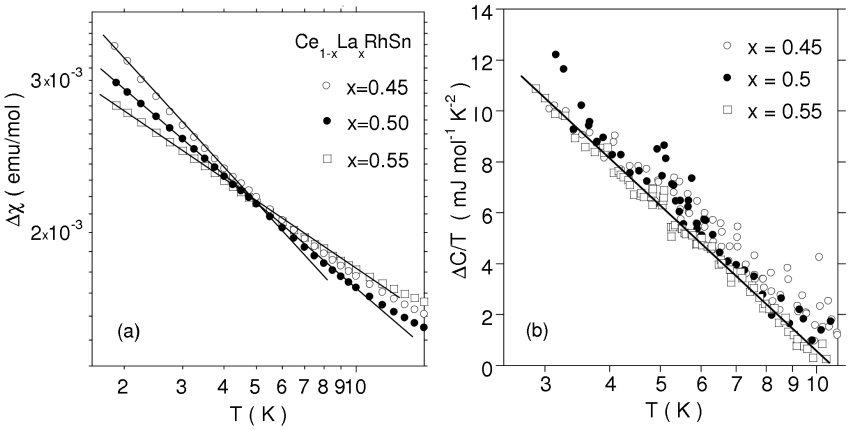


Fig. 2. Temperature variation of the zero-field cooling (ZFC) magnetic susceptibility $\Delta\chi$ on a double-logarithmic plot for $Ce_{1-x}La_xRhSn$ compounds (a). In (b) $\Delta C/T$ vs. $\ln T$ for $Ce_{0.55}La_{0.45}RhSn$, $Ce_{0.5}La_{0.5}RhSn$, and $Ce_{0.45}La_{0.55}RhSn$.

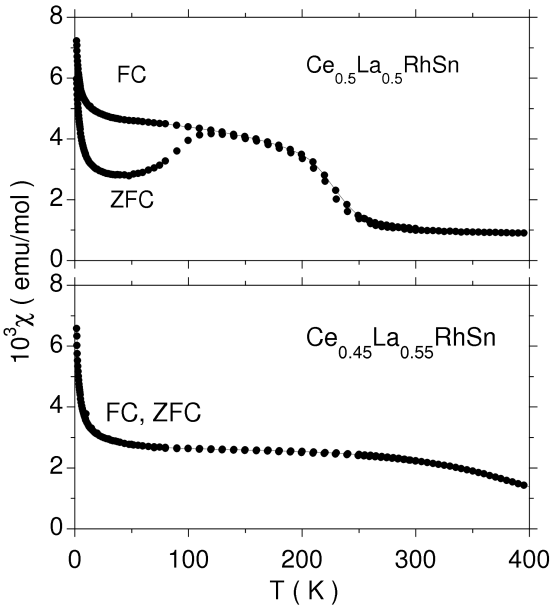


Fig. 3. FC and ZFC susceptibility $M/H$ vs. $T$ in a magnetic field of 0.5 T for $Ce_{1-x}La_xRhSn$ near the critical concentration $x_c \approx 1/2$.

for the carrier concentration $n_c$ for $x \leq x_c$ created by their thermal excitation across the Kondo gap $2\Delta$. Also, we have found that the collective Kondo-singlet is destroyed for doping when $x > x_c$ or at $T > T_m$, where $T_m$ is the temperature of the maximum in $\chi(T)$ experimentally obtained for the components $x \leq 0.12$ ($T_m \approx 19$ K for CeRhSb and it is decreasing while increasing $x$ in the concen-

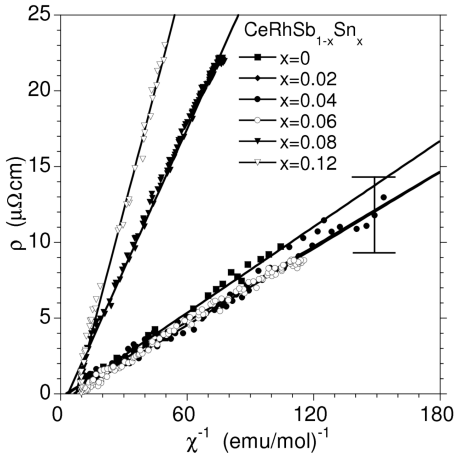


Fig. 4. Linear scaling law between the resistivity $\rho$ and the susceptibility $\chi$ for the nonvanishing Kondo gap. The values of $\chi$ and $\rho$ for different $x$ are shifted to the zero values at the minimal positions (details in Ref. [22]).

tration region $x \leq 0.12$). The resistivity $\rho(T)$ data show a maximum at $T_{\max}$ resulting from a competition between quantum coherence (itineracy of $4f$ electrons setting in upon cooling) and the thermal disorder acting as a decoherence factor leading to the localization of the $4f$ states above $T_{\max}$ (details in Ref. [22]). In the concentration region $x \leq 0.12$ the $\rho(T)$ and $\chi(T)$ data indicate that the $f$ electrons are itinerant between $T_{\rm m}$ and $T_{\max}$, whereas for $T < T_{\rm m}$ the collective spin-singlet state formation results in reentrant $4f$-electron localization upon cooling the system.

On the Sn-rich side we observe both the singular quantum fluctuations associated with the $4f$ electrons (on the low-energy scale) and the Rh $4d$ spin fluctuations at higher temperatures. The specific heat data (Fig. 5) in the range $6 < T < 25$ K are well fitted by expression $C/T = \gamma^* + \delta T^2 \ln(T/T_{\rm sf})$ characteristic of the spin fluctuations; $\gamma^*$ is the linear specific heat coefficient containing the mass enhancement, and $T_{\rm sf}$ is the spin-fluctuation temperature.

We also note that in Fig. 5 the same parameters obtained for LaRhSn fit well the $C/T$ data for CeRhSn and $CeRhSb_{1-x}Sn_x$, where $x \geq 0.78$, which suggests the high temperature spin-fluctuation contribution from the presence of Rh atoms. Let us note also that the electronic structure of CeRhSn and LaRhSn, that generally decides about the thermodynamical and electric transport properties of solids, is quite different. In Fig. 6 we compare the density of states (DOS) for both compounds, obtained from the linear muffin-tin orbital (LMTO) calculations [23]. The total DOSs are compared in the figure with the respective valence band X-ray photoelectron spectra (XPS). In our opinion, a very similar Rh DOS either in CeRhSn or LaRhSn support the observation about the role of the spin-fluctuation contribution from the Rh atoms in the specific heat.

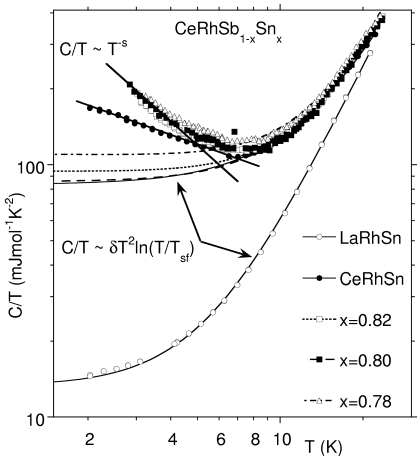


Fig. 5. The specific heat $C/T$ data fitted to the spin-fluctuation formula $C/T = \gamma^* + \delta T^2 \ln(T/T_{\rm sf})$ in the higher temperature ($6.5 < T < 23$ K) region. For Ce-compounds the fitting parameters are very similar: $\gamma^*$ is about 90 mJ/(mol K$^2$) and $T_{\rm sf}$ is $\approx 0.9$ K. At low temperatures, $C/T \sim T^{-s}$ (the straight lines are the fits plotted in the log-log scale). The fitted curve for LaRhSn is also included for comparison ($\gamma^* = 13.3$, $T_{\rm sf} = 0.43$ K). For LaRhSn the parameters were obtained from the fit in the range of $1.9 \div 25$ K. The straight lines for $T < 6$ K represent the power-law dependences, whereas the flat parts below them are the extrapolation tails of the spin-fluctuation formula (details in Ref. [22]).

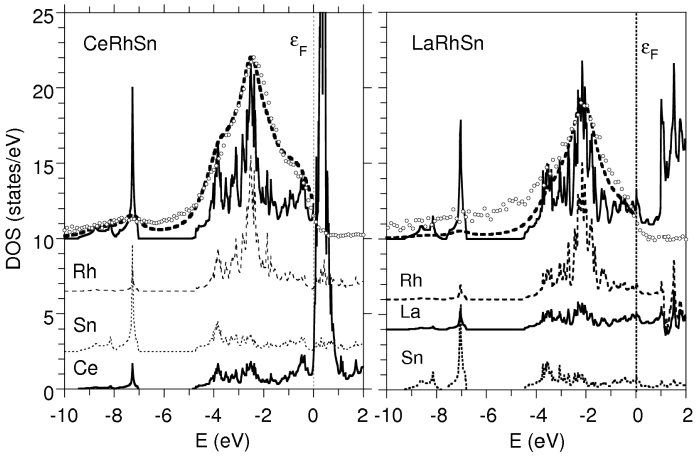


Fig. 6. Comparison of the total DOS calculated for CeRhSn, convolved by Lorentzians of half-width 0.4 eV, taking into account proper cross-sections for bands with different $l$ symmetry (thick curve), and the measured XPS valence bands for CeRhSn and LaRhSn, respectively, corrected by the background. The partial DOS curves are plotted below.

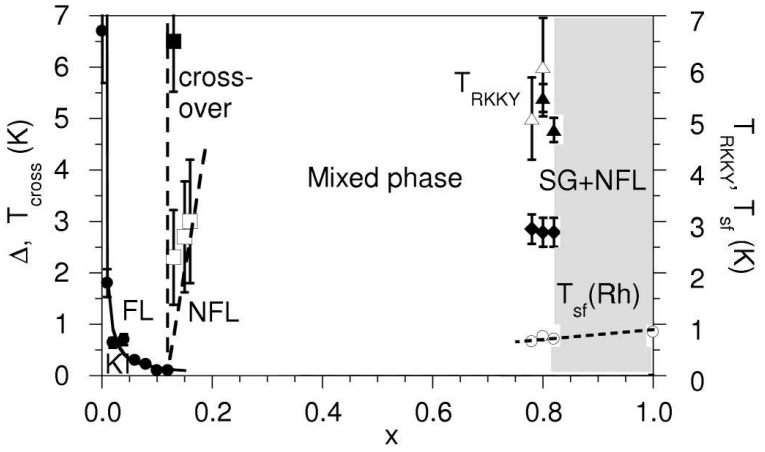


Fig. 7. Phase diagram for $CeRhSb_{1-x}Sn_x$ system. Solid points on the left mark the values of the Kondo gap. At the Sb-rich side the full square marks the deviation point from the $T^2$ dependence of resistivity for the sample $x = 0.13$, whereas the open squares mark the disappearance points of a very weak hysteresis of the magnetization curves appearing at low $T$ (see Ref. [22]). The part for $x > 0.78$ displays spin-fluctuation temperature $T_{\rm sf}$ which characterizes $4d$ electron fluctuations, obtained from the specific heat. $T_{\rm RKKY}$ for the Sn-rich side of this diagram is taken from the ac susceptibility data as the temperature of weak maximum in the $\chi(T)$ plot [29]. Open triangles mark $T$ at which magnetization $M(H)$ deviates from linearity (details in Ref. [29]). SG+NFL denotes a coexistence of an itinerant $4f$ electron spin-glass state with NFL behavior.

In the low-$T$ regime $T < 6$ K, $C/T$ has the power-law dependence $T^{-s}$. The energy scale of the two processes: the spin-fluctuation contribution due to the $4d$ electrons and the singular quantum fluctuation coming from the Ce $4f$ electrons are well separated and this allows us to differentiate between them. Those fluctuations coexist with a weak magnetic order among itinerant electrons, probably of mainly $4f$ character [29]. On the basis of our experimental results we present in Fig. 7 a schematic phase diagram for $CeRhSb_{1-x}Sn_x$ on the $T-x$ plane.

## 3. Concluding remarks

In conclusion, the most spectacular in our studies [22, 29] was the observation of quantum criticality at the border of Kondo insulator–non-Fermi liquid as a function of a number of valence electrons in the correlated electron $CeRhSb_{1-x}Sn_x$ system. In Fig. 7 the diagram displays for $0.12 < x < 0.2$ at the Sb-rich side the crossover region from either KI or Fermi liquid states to the non-Landau NFL metallic phase. Doradziński and Spałek (DS) discussed the possible magnetic phases in the periodic Anderson model and determined the conditions under which there appears a heavy-fermion and the Kondo insulating liquid states [30]. The

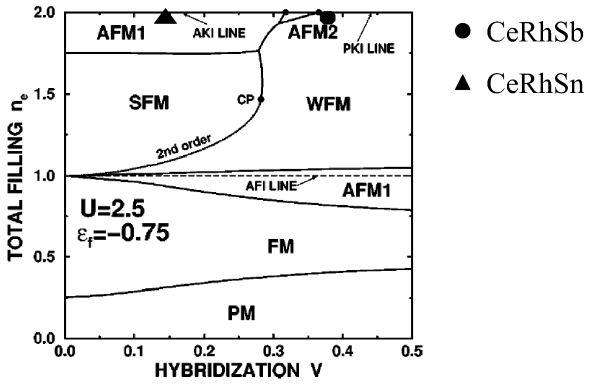


Fig. 8. DS phase diagram (details in Ref. [30]). FM, WFM, and SFM are ferromagnetic, weakly ferromagnetic, or strongly ferromagnetic metallic phases, respectively. AFM are different antiferromagnetic metallic phases, and PKI or AKI are paramagnetic or antiferromagnetic Kondo insulators, respectively. The points represent the experimental data for the Kondo lattices CeRhSn and CeRhSb, which are experimentally obtained from the 3*d* Ce XPS spectra [31].

stability of paramagnetic vs. magnetic ground state in the Kondo-lattice limit is strongly dependent on the hybridization energy $V$, the bare $f$-level position, the number of electrons $n_{\rm e} = n_f + n_{\rm c}$, and on the intrasite $f-f$ Coulomb interaction $U$. In the DS phase diagram (see Fig. 8), CeRhSn is obtained as a weak antiferromagnetic metal [31], which evolves into a paramagnetic Kondo insulator (the case of CeRhSb) with increasing $V$. Both CeRhSn and CeRhSb have the total number of relevant valence electrons $n_{\rm e} \approx 2$ (for CeRhSb we have estimated that $n_{\rm e} > 1.8$, whereas for CeRhSn $n_{\rm e}$ it is about 1.7). On the $V-n_{\rm e}$ line the DS diagram suggests the critical behavior for $V \approx 0.35$ eV, which was confirmed experimentally from the 3*d* Ce XPS spectra.

## Acknowledgments

The authors acknowledge the financial support of the Ministry of Science and Higher Education, grants Nos. 1 P03B 052 28 and 1 P03B 001 29. J.S. thanks also the senior fellowship of the Polish Foundation for Science for the years 2003–2007. This work was performed under the auspices of the COST P-16 European Network entitled "Emergent Behaviour in Correlated Matter".

## References

[1] J. Kondo, *Prog. Theor. Phys.* **32**, 37 (1964).

[2] A.S. Edelstein, *Phys. Rev. Lett.* **20**, 1348 (1968).

[3] J.M. Lawrence, P.S. Reiseborough, R.D. Parks, *Rep. Prog. Phys.* **44**, 1 (1981).

[4] G.R. Stewart, *Rev. Mod. Phys.* **56**, 755 (1984).

[5] F. Steglich, J. Aarts, C.D. Bredl, *Phys. Rev. Lett.* **43**, 1892 (1979).

[6] Z. Fisk, J.L. Sarro, J.D. Thompson, D. Mandrus, M.H. Hundley, A. Miglori, B. Bucher, Z. Schlesinger, G. Aeppli, E. Bucher, J.F. DiTusa, C.S. Oglesby, H.R. Ott, P.C. Confield, S.E. Brown, *Physica B* **206/207**, 798 (1995).

[7] G.R. Stewart, *Rev. Mod. Phys.* **73**, 797 (2001).

[8] J.A. Hertz, *Phys. Rev. B* **14**, 1165 (1976).

[9] C.L. Seaman, M.B. Maple, B.W. Lee, S. Ghamaty, M.S. Torikachwili, J.-S. Kang, L.Z. Liu, W. Allen, D.L. Cox, *Phys. Rev. Lett.* **67**, 2882 (1991).

[10] H. v. Löhneysen, T. Pietrus, G. Portisch, H.G. Schlager, A. Schröder, M. Siech, T. Trappmann, *Phys. Rev. Lett.* **72**, 3262 (1994).

[11] O.O. Bernal, D.E. MacLaughlin, H.G. Lukefahr, B. Andraka, *Phys. Rev. Lett.* **75**, 2023 (1995).

[12] E. Miranda, V. Dobrosavljevic, G. Kotliar, *J. Phys., Condens. Matter* **8**, 9871 (1996).

[13] N.D. Mathur, F.M. Grosche, S.R. Julian, I.R. Walker, D.M. Freye, R.K.W. Haselwimmer, G.G. Lonzarich, *Nature* **394**, 39 (1998).

[14] F.M. Grosche, P. Agarwal, S.R. Julian, N.J. Wilson, R.K.W. Haselwimmer, S.J.S. Lister, N.D. Mathur, F.V. Carter, S.S. Saxena, G.G. Lonzarich, *Nature* **394**, 39 (1998).

[15] P. Gegenwart, F. Kromer, M. Lang, G. Sparn, C. Geibel, F. Steglich, *Phys. Rev. Lett.* **82**, 1293 (1999).

[16] P. Coleman, A.J. Schofield, *Nature* **433**, 226 (2005).

[17] M.B. Maple, M.C. de Andrade, J. Herrmann, Y. Dalichaouch, D.A. Gajewski, C.L. Seaman, R. Chau, R. Movshovich, M.C. Aronson, R. Osborn, *J. Low Temp. Phys.* **99**, 223 (1995).

[18] M.B. Maple, R.P. Dickey, J. Herrmann, M.C. deAndrade, E.J. Freeman, D.A. Gajewski, R. Chau, *J. Phys., Condens. Matter* **8**, 9773 (1996).

[19] O. Trovarelli, C. Geibel, S. Mederle, C. Langhammer, F.M. Grosche, P. Gegenwart, M. Lang, G. Sparn, F. Steglich, *Phys. Rev. Lett.* **85**, 626 (2000).

[20] A. Ślebarski, M. Radlowska, T. Zawada, M.B. Maple, A. Jezierski, A. Zygmunt, *Phys. Rev. B* **66**, 104434 (2002).

[21] A. Ślebarski, A. Czopnik, A. Zygmunt, T. Zawada, *J. Phys., Condens. Matter.* **16**, 4897 (2004).

[22] A. Ślebarski, J. Spałek, *Phys. Rev. Lett.* **95**, 046402 (2005); J. Spałek, A. Ślebarski, J. Goraus, L. Spałek, K. Tomala, A. Zarzycki, A. Hackemer, *Phys. Rev. B* **72**, 155112 (2005).

[23] A. Ślebarski, A. Jezierski, M.B. Maple, A. Zygmunt, *Acta Phys. Pol. B* **32**, 3331 (2001); A. Ślebarski, M.B. Maple, E.J. Freeman, C. Sirvent, M. Radłowska, A. Jezierski, E. Granado, Q. Huang, J.W. Lynn, *Philos. Mag. B* **82**, 943 (2002); P.-C. Ho, V.S. Zapf, A. Ślebarski, M.B. Maple, *Philos. Mag.* **84**, 2119 (2004).

[24] R.B. Griffiths, *Phys. Rev. Lett.* **23**, 17 (1969); A.H. Castro Neto, G. Castilla, B.A. Jones, *Phys. Rev. Lett.* **81**, 3531 (1998).

[25] A. Ślebarski, K. Szot, M. Gamża, H. Penkalla, U. Breuer, *Phys. Rev. B* **72**, 85443 (2005).

[26] A. Ślebarski, K. Grube, R. Lortz, C. Meingast, H. v. Löhneysen, *J. Magn. Magn. Mater.* **272-276**, 234 (2004).

[27] S.K. Malik, D.T. Adroja, *Phys. Rev. B* **43**, 6277 (1991).

[28] A. Ślebarski, T. Zawada, J. Spałek, A. Jezierski, *Phys. Rev. B* **70**, 235112 (2004).

[29] A. Ślebarski, J. Spałek, M. Gamża, A. Hackemer, *Phys. Rev. B* **73**, 205115 (2005); A. Ślebarski, N.A. Frederick, M.B. Maple, *Philos. Mag.* **82**, 1275 (2002).

[30] J. Spałek, R. Doradziński, in: *Magnetism and Electronic Correlations in Local--Moment Systems: Rare Earth Elements and Compounds*, Eds. M. Donath, P.A. Dowben, W. Nolting, World Scientific, Singapore 1998, p. 387; R. Doradziński, J. Spałek, *Phys. Rev. B* **58**, 3293 (1998); for brief review see: J. Spałek, R. Doradziński, *Acta Phys. Pol. A* **96**, 677 (1999); *ibid.* **97**, 71 (2000).

[31] A. Ślebarski, *J. Alloys Comp.* **423**, 15 (2006); A. Ślebarski, J. Spałek, *J. Magn. Magn. Mater.* **310**, e85 (2007).